Available online at www.sciencedirect.com
ScienceDirect
Journal of Sound and Vibration 304 (2007) 186–200
JOURNAL OF SOUND AND VIBRATION
www.elsevier.com/locate/jsvi

Instability of systems with a frictional point contact—Part 3: Experimental tests

P. Duffour[a], J. Woodhouse[b,*]

[a]University College London, Department of Civil and Environmental Engineering, London WC1 6BT, UK
[b]University of Cambridge, Department of Engineering, Cambridge CB2 1PZ, UK

Received 5 January 2006; received in revised form 13 February 2007; accepted 14 February 2007

Abstract

In two earlier papers, a new formalism was derived which led to the prediction of instability for two linear systems in sliding contact at a single point. In Duffour and Woodhouse [Instability of systems with a sliding point contact. Part 1: basic modelling 271 (2004) 365–390], predictions were obtained using a friction law featuring a constant coefficient of friction. This formalism was generalised in Duffour and Woodhouse [Instability of systems with a sliding point contact. Part 2: model extensions 271 (2004) 391–410] to include all possible linear routes to instability. This paper presents results from the experimental investigation carried out to test the validity of the theoretical results obtained in the first of the two papers. The rig is of the pin-on-disc type. An instrumented pin was specially designed so that the quantities necessary for the prediction could be measured. It emerged that incipient squeal frequencies observed experimentally could be predicted in 75% of the cases using the simplest formalism presented in Duffour and Woodhouse (2004). The presence of unpredicted squeal frequencies points towards the importance of other effects, such as the disc nominal rotation speed and the value of the normal preload. This study also reveals that the ever-changing nature of friction-induced noises can, to a good extent, be explained by the slight structural variations undergone by any mechanical system.

1. Introduction

When two solid surfaces slide against each other, the friction force which resists the sliding motion can cause the system to vibrate. Although this phenomenon is extremely familiar and wide ranging [1]—from machine chatter, to brake noise or bowed musical instruments—it is still poorly understood. In two previous papers [2,3], a theory was presented which allows the modelling of instability occurring when *two vibrating systems* are coupled through *a single sliding point contact*. The dynamics of the two mechanical subsystems are supposed to be *linear*. At the contact point, friction arises due to relative sliding of the two subsystems. In these two papers, two friction laws were investigated: Coulomb's law with a constant coefficient of friction [2], and a friction law where the coefficient of friction varies linearly with the sliding velocity [3]. Unlike most studies of brake noise, the dynamics of the system were not modelled by a specific lumped-parameter model. Instead the mechanical

*Corresponding author. Fax: +44 01223 332662.
E-mail addresses: p.duffour@ucl.ac.uk (P. Duffour), jw12@eng.cam.ac.uk (J. Woodhouse).

0022-460X/$ - see front matter © 2007 Elsevier Ltd. All rights reserved.
doi:10.1016/j.jsv.2007.02.019

behaviour of the two subsystems was described by appropriate transfer functions. Therefore, no particular assumption is made about the physical realisation of the components, although all their relevant mechanical characteristics (mass, damping, stiffness) are captured by the transfer functions. Using these transfer functions and the coefficient of friction between the two sliding bodies, the theory predicts the modal frequencies of the coupled system as well as the stability of the corresponding modes.

This paper describes experimental testing of the theory presented in the first theoretical paper. The experimental rig belongs to the pin-on-disc category. One of the subsystems is a rotating disc, which provides the sliding motion. The other subsystem is a 'pin' of a special design, incorporating sensors so that the coefficient of friction can be estimated during a run. For the prediction of the frequencies of instability—"squeal" in brake terms—the simplest version of the theory presented in Ref. [2] is used. This requires (1) measurements of the point admittance transfer function matrices **H** for the pin and **G** for the disc, defined at the contact point; and (2) the value of the coefficient of friction. Once these are known, it was shown that the frequencies of instability for the coupled system are the zeros of a certain function D, when they are located in the lower half-complex plane.

2. Description of the experimental apparatus

2.1. General overview of the rig

Fig. 1(a) is a side view photograph of the complete pin-on-disc assembly as it is during a squeal test. A schematic drawing of the setup is shown in Fig. 1(b). Both figures show the pin subsystem (right) in contact with the disc (left) in running configuration. The disc lies in a vertical plane and the contact point on the disc is located towards the outer rim, along a horizontal diameter. Therefore, when the disc is rotating, the normal force and displacement are in the horizontal axial direction, while the tangential force and displacement are in the vertical direction.

The disc used was made of aluminium. It was annular with the following dimensions and mechanical properties:

$$\text{Outer diameter } R_o = 258\,\text{mm} \quad \text{Young's modulus } E = 70.3\,\text{GPa}$$
$$\text{Inner diameter } r_o = 23\,\text{mm} \quad \text{Poisson's ratio } \nu = 0.3$$
$$\text{Thickness } h = 11\,\text{mm} \quad \text{Density } \rho = 2700\,\text{kg/m}^3.$$

The pin assembly can be divided into three main parts: first, a bulky square bracket mounted on leaf springs (right and lower part in each figure); second, a top-hat dynamometer: this is the part that comes in contact with the disc; and third, a flexible strip arrangement used to mount the top-hat cylinder onto the supporting bracket. The support bracket is made of thick steel plates welded together at right angles (with thinner

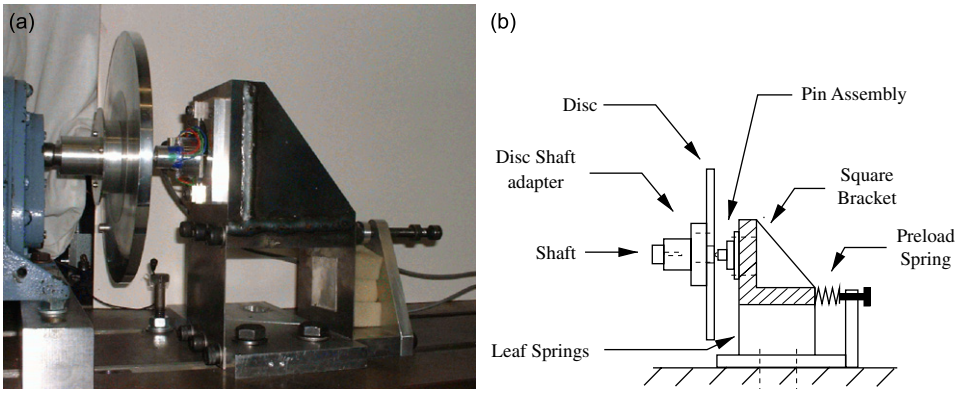

Fig. 1. (a) Photograph showing the whole pin-on-disc assembly in running condition. The pin assembly (right) is in contact with the rotating disc (left) through a rounded tip. (b) Side view diagram describing schematically the main parts of the rig visible in the photograph.

reinforcement plates on each side). It is designed to be as rigid as possible, in the frequency range of interest, compared to other components of the pin assembly. The whole pin subsystem is clamped to a heavy machine table by an aluminium base plate; the bracket is linked to the base plate through two leaf springs. This allows the dynamometer-bracket assembly to move almost freely in the horizontal (i.e. normal) direction, while almost completely preventing rigid body motion of the whole assembly in the vertical (i.e. tangential) direction and indeed in any other degrees of freedom. A horizontal spring can be pushed against the back of the square bracket, allowing the pin subsystem to be preloaded against the disc. This preloading spring is partly visible on the right-hand side of Figs. 1(a) and (b). A normal preload is necessary for the tip of the pin to remain in contact with the disc. It ensures that the pin assembly tracks the deflection of the disc due to any misalignments. From a dynamical point of view, the preloading spring amounts to an extra stiffness element in parallel with the leaf springs. The rigid body mode of the bracket on leaf spring could easily be identified around 20 Hz, well below the other modes of the system.

The top-hat dynamometer is an axisymmetrical solid made out of a single block of Dural. A schematic drawing of this top-hat together with the attachment to the bracket is shown in Fig. 2 (transducers not shown). The dynamometer makes contact with the disc through a rounded tip. A tip made of whichever friction material is desired can be screwed to the end of the top-hat cylinder as shown in Fig. 2. The most important part of the top-hat element is the thin cylindrical shell. At its base this thin shell merges into a much thicker cylinder which contains holes for attachment. Given the thinness of the cylindrical shell (0.75 mm), it can be considered as the first compliant mechanical element viewed from the contact point. This compliance is used to measure the normal and friction forces at the contact point. Following Smith [4, p. 22], arrangements of strain gauges were fitted to the cylindrical shell to measure the normal and friction forces. Strain gauges have a poor signal to noise ratio but they have the advantage of being extremely light, and allow measurements down to DC values which is essential for this application. In all, eight gauges were fitted on the shell, one full bridge for each force. For this application, pairs of 120 Ω gauges, mounted at 90° on a 2 mm rosette were used (model FCA-2-23 from TML). The out-of-balance signals were conditioned by two Fylde amplifiers (FE-H359-TA) having a bandwidth from DC to 50 kHz. The normal force was measured by gauges aligned along the axis of the cylinder. The friction force induces pure shear stresses along the horizontal plane of symmetry of the shell which was measured using gauges rotated by 45° with respect to the axis of cylinder.

The output signals from the two Fylde amplifiers were calibrated statically by hanging known weights in both directions in turn. Besides the required calibration factors, this test confirmed that the linearity of the transducers is very good, and that the strains in the two directions are reasonably well decoupled (less than 5% within the calibrated range). Because of problems of insensitivity and bridge balancing, the accuracy of F and N cannot be guaranteed at better than 5%.

To provide suitable dynamics of the pin assembly, the dynamometer was fixed to the bracket via a flexible strip as shown in Fig. 2. The top-hat cylinder is bolted to the strip at two points. The strip is then screwed to a much thicker aluminium plate. This plate allows the strip and the top-hat assembly to be fixed onto the heavy

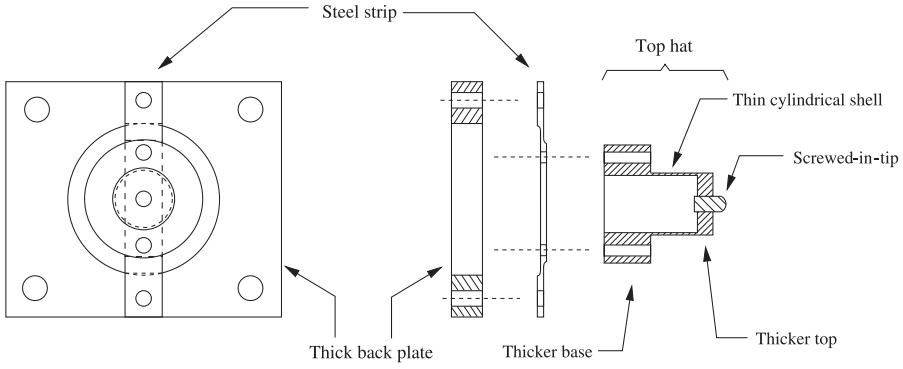

Fig. 2. Schematic drawing of the top-hat dynamometer and its attachment system. Front view and split section of the mounting assembly. The dashed lines show the location of the bolts. The thick back plate is clamped to the square bracket by four bolts on each corner of the plate. The contact tip is screwed at the end of the cylindrical shell.

square bracket described above. The steel strip was machined carefully to avoid sharp corners and consequential high local stresses at the regions in contact, either with the top hat or with the back plate. Although the cylindrical shell of the dynamometer is thin, the whole top hat is much stiffer than the steel strip. The shell is thin enough to measure the strain induced by the contact forces but it is thick enough to make the top hat much less compliant than the steel strip.

The theory presented in Ref. [2] shows that instability can only occur if there is a non-zero coupling between normal and tangential motion in either or both of the two uncoupled subsystems. Since the disc is almost perfectly symmetrical, such coupling can only be present if the top hat is not positioned symmetrically on the metal strip. To ensure that the coupled system has unstable zeros, asymmetry was deliberately introduced in the pin assembly by attaching the top hat on the strip about 10 mm away from the middle of the strip (although it is shown in a central position in Fig. 2).

2.2. Dynamic properties of the pin assembly

The theory presented in Ref. [2,3] requires the measurement of one 2×2 mobility transfer function matrix for each subsystem. This matrix was denoted **H** for the pin subsystem. The velocities were measured using a laser vibrometer Polytec OFV 056 Sensor Head driven by a Polytec OFV 3001 S Controller. The structure was excited by a piezoelectric impulse hammer PCB 484B11. All the transfer functions shown here have been filtered using a low-pass filter at 30 kHz embedded in the Polytec vibrometer system. For the experimental procedure to be repeatable, it was important not to damage the disc surface irreversibly during a squeal test. Therefore, only tips made of Perspex (PMMA) were used. Measuring the transfer functions **H** requires hitting the assembly at the tip with the impulse hammer. Polymer tips would prevent the excitation of higher frequencies, therefore the transfer functions were measured using a different tip made of steel but otherwise similar to the polymer tips.

All the transfer functions in **H** require exciting the subsystem and measuring its response at the same point—the point of contact during a squeal run. For the cross-terms H_{12} or H_{21}, exciting one side of the tip while measuring in the perpendicular direction gave good results. For the driving point transfer function H_{11} the tip was excited and the response measured by pointing the laser at the back of the tip. Appropriate holes were made in plates at the back of the device to allow the laser beam to pass through. All the pin transfer functions were measured with the preloading spring applied so that the leaf springs are ''sprung''. However, as the tip is not in contact with the disc, the steel strip on which the top hat is mounted is not stressed by this preloading (as it would if the pin assembly was pushing onto the disc).

Fig. 3 shows the four transfer functions. Each transfer function is the average of 40 measurements. The sampling frequency was 100 kHz. Using other measurements not shown here, it was possible to identify the first two peaks, appearing on the plot at 945 and 2800 Hz, as the first and second bending mode of the strip. The normal driving point transfer function H_{11} also contains a strong lower peak at 20 Hz, corresponding to the rigid body mode of the bracket on leaf springs. Plotting the four transfer function shows clearly that the peak at 11.7 kHz is mainly a lateral mode whereas the mode just above 20 kHz is mainly normal. These two higher modes could not be related to any strip mode with certainty, but it seems plausible that they are the two next strip modes. Measuring the driving point transfer function in the transverse direction (i.e in the plane of the strip but perpendicular to the longitudinal direction of the strip) confirmed that they were not torsional modes as those were clearly identified at 500 Hz and 13.2 kHz (and no others up to 25 kHz).

The frequency shift produced by the mass difference between the tip made of steel and that made of perspex was corrected by carrying out an impact test with the polymer tips. This provided an accurate measurement of the actual natural frequencies of the pin assembly in operating condition. The shift in frequency is up to 6% for the first 5 modes. It is possible that this difference in mass also slightly modifies the values of the mode shape coefficients, but these were kept unchanged: if, for a given pin transfer function, the measurements with the two different tips (steel and polymer) are plotted together, the peak amplitudes appear hardly affected.

The pin subsystem thus appears to have only four main normal and/or tangential modes in the range 0–20 kHz. Therefore the objective of designing a pin subsystem with clear and unambiguous dynamics has been achieved. The asymmetry in the geometry of the assembly ensures that the cross-terms of the pin transfer function matrix H_{21} or H_{12} are significant compared to the diagonal transfer functions H_{11} and H_{22}.

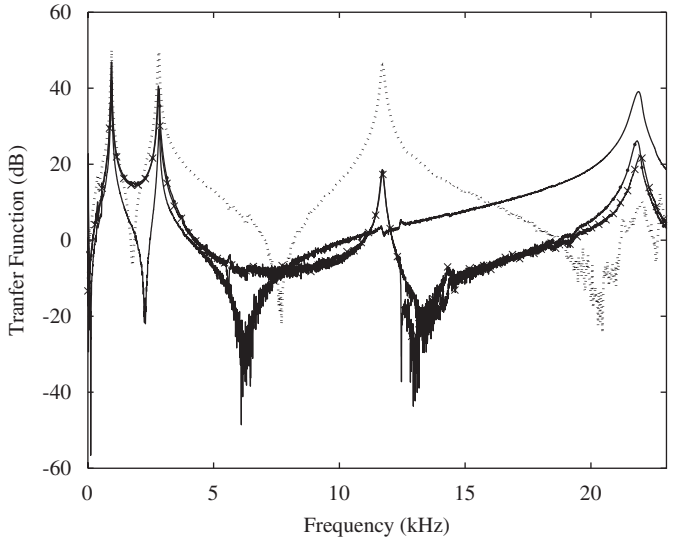

Fig. 3. Set of transfer functions constituting the matrix **H** for the pin subsystem. Solid line: G_{11}; dotted line: G_{22}; Solid with dots: G_{12}; Solid with crosses: G_{21}.

2.3. Dynamics of the disc subsystem

The admittance transfer function matrix of the disc subsystem was denoted **G** in Ref. [2,3]. G_{11} is the transfer function for the response of the disc in the normal direction to an excitation in the normal (i.e. out-of-plane) direction. This was measured with the laser pointing at the back of the disc while the hammer was hitting the disc on the other side at the same radial and angular position. The radius at which the transfer functions was measured was $r_1 = 120$ mm, which is also the location where the pin is in contact with the disc during a squeal test.

To be able to measure the response and to excite the disc in the lateral direction, a small stud was screwed to the back of the disc, again at a radius of 120 mm from the centre of the disc. The laser was pointed at the stud, tangentially to the trajectory of the stud when the disc is rotating. The stud was hit by the hammer in the opposite direction. The value of G_{22} measured in this way must be compensated for the fact that the stud projects out of the disc surface. The cross admittances G_{12} and G_{21} were measured and compensated in a similar way. The transfer functions G_{11} and G_{22} are shown in Fig. 4. Each was obtained by averaging 40 measurements.

Comparison with results of a standard modal test carried out using the scanning laser vibrometer and a Finite Element model of the annular disc (ABAQUS) allowed most of the peaks in Fig. 4 to be identified: each is labelled by two numbers, first the number of nodal diameters, then the number of nodal circles. 'IP' labels the In-plane modes. The plot shows clear peaks, most of them very lightly damped. A clear peak around 600 Hz is a good candidate for mode (0,0), although this could also be a strong bending mode of the shaft supporting the disc system. However (0,1) and (0,2), expected around 2400 and 9700 Hz, respectively, are not visible in this plot of G_{22} (they are not expected to be visible on G_{11}). A possible explanation for this absence is that the stud may be located close to a nodal circle. Within the range displayed, three in-plane modes can clearly be identified (in G_{22} only) at the frequencies 8750, 14 580 and 16 255 Hz. They match the FE prediction.

G_{12} and G_{21} were also measured and were found to be extremely small compared to the diagonal transfer functions of the admittance matrix (at between 30 and 40 dB lower). This confirms the claim made in Ref. [2] that symmetry in the disc causes the normal and tangential degrees of freedom to be effectively decoupled. The presence of the stud however reduced the disc symmetry slightly and caused each diametral doublet mode to be split as explained by Rayleigh [5, Section 221].

Split modes could be important for friction instability. Some authors (e.g. [6,7]) have argued that brake noise results from 'flutter instability', and that 'flutter instability' means 'coalescence' of two eigenvalues of the

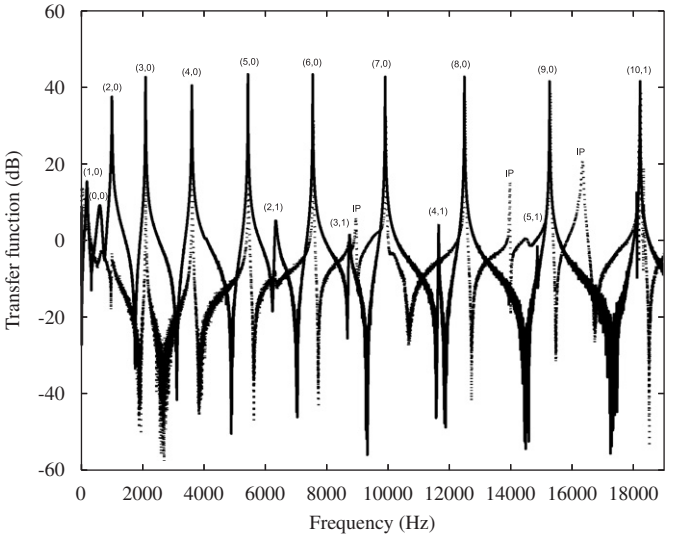

Fig. 4. Transfer functions G_{11} (solid line) and G_{22} (dotted line). The modes are labelled according to the convention: (diameter,circle). 'IP' means 'In-Plane' mode; those are only visible in G_{22}.

system when a parameter is varied (bifurcation). Doublet modes are good candidates for coalescence since their frequencies are already very close.

3. Prediction of the unstable frequencies

The last two sections described how the transfer function matrices—**H** for the pin and **G** for the disc—and how the contact forces F and N were measured. The coefficient of friction $\mu_\circ$ was estimated experimentally from these by division and smoothing to get quasi-static values. For the purpose of prediction, constant values of $\mu_\circ$ were used, varied over a range which included all the measured values, as explained in Section 3.3. The theory developed in Ref. [2] predicts that the system is unstable when the function D defined by

$$D(\omega) = G_{11} + H_{11} + \mu_\circ[H_{12} + G_{12}] \tag{1}$$

has one or more zeros in the lower half-complex plane. As $G_{12} \approx 0$ (see Section 2.3), only G_{11}, H_{11} and H_{12} are required for this theory. In this case, the disc only influences the instability prediction through its normal–normal component G_{11}. Further investigation allowing the coefficient of friction to vary with the sliding speed [3] would need the other transfer functions too.

An experimental transfer function is a complex-valued function of the real variable ω. If the experimental values of the transfer functions were directly used in Eq. (1), it would not be possible to evaluate $D(\omega)$ for complex ω. However the zeros of D could lie anywhere in the complex plane. To be able to find the non-real zeros of D, it is therefore necessary to obtain a mathematical expression for the various experimental transfer functions first. Fitting the transfer functions measured experimentally also has the additional advantages that the data is rid of any noise and that a large amount of data is replaced by a limited number of parameters.

Provided a vibrating system is linear a transfer function can be expected to take the form (see e.g. Ref. [8]):

$$H_n(\omega) = \sum_{k=1}^{m} \left[\frac{c_{kn}}{\omega - \overline{\omega}_k} + \frac{c_{kn}^*}{\omega + \overline{\omega}_k^*} \right], \tag{2}$$

where ω is the frequency, $\overline{\omega}_k = \omega_k(1 + 2i/Q_k)$, ω_k and Q_k are the kth undamped natural frequency and Q-factor, respectively; c_{kn} is the residue for the kth mode for transfer function n; * denotes complex conjugate, and m is the number of modes within the frequency range considered. Fitting a transfer function requires choosing the values of ω_k, Q_k and c_{kn} so that the theoretical curve becomes as close as possible to the experimental one.

The method used for fitting was a global multi-degree of freedom algorithm originally implemented for a previous project [9] and further improved by Adhikari [10] following the general principles outlined in Ref. [11]. The final result for the fitting of G_{11} by this method is shown in Fig. 5.

This plot shows that a very good fit was eventually obtained as the two curves appear almost superimposed. The result is only shown for G_{11} because it was by far the most difficult case as it contains many modes, with very different amplitudes and occasionally with moderate overlap. This transfer function (G_{11}) was fitted using only one frequency for each doublet mode. Equally good fitting could be obtained for all required transfer functions.

3.1. The zero-finding procedure

For both subsystems, transfer functions were fitted up to 19 kHz (this particular frequency was chosen because there was a cluster of large amplitude peaks around 18 kHz which it was thought best to include). Once the complex frequency and amplitude vectors are known from fitting, the transfer functions are a sum of simple first-order rational fractions. From Eq. (1), it is clear that this is also the case for $D(\omega)$. A Matlab program then computes the coefficients of the polynomial $P(\omega)$ defined as the numerator of $D(\omega)$ when D is written as a single ratio of two polynomials $D(\omega) = P(\omega)/Q(\omega)$. The zeros of $D(\omega)$ are then found using Matlab's root extraction routine on $P(\omega)$. This provides a set of complex zeros which can be plotted in the complex plane.

In order to verify the soundness of the numerical scheme, the predicted zeros were monitored for an increasing number of uncoupled modes included in D. Results showed that by included uncoupled modes up to 19 kHz, one obtained converged and stable zeros in the audio range ($\leqslant$15 kHz).

3.2. Outline of the testing procedure

Experiments in friction-induced vibration are notoriously difficult because they usually offer very poor repeatability, even under apparently identical external conditions. The behaviour of the rig presented in this paper is no exception to this rule. This makes the task of testing a theory particularly delicate: the formalism presented in Ref. [2] yields definite predictions of unstable frequencies which are difficult to test against the sporadic occurrence of various noise frequencies. To investigate in a somewhat systematic way the behaviours that the rig could exhibit, a standard set of noise tests was carried out every day over a week. These noise tests will be described in detail in Section 4 but in essence, they involve monitoring the sound emitted and the contact forces while the pin is pushed in contact with the rotating disc. Ideally, the subsystem transfer functions should be measured as close in time as possible to the noise tests. However this proved impractical. As a compromise, the transfer function matrices were measured twice: once at the start and once at the end of

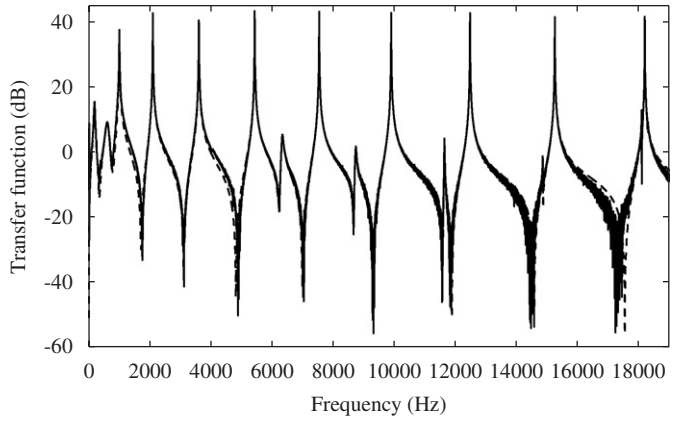

Fig. 5. Fitting of G_{11}. The solid line is the original data; the dashed line shows its fitted version.

the week of measurement. The transfer functions shown so far are taken from the second and final set of measurements.

From the two sets of measured transfer functions, it was possible to predict two sets of unstable frequencies for the coupled system. Before showing these predictions, it is instructive to examine how the modal parameters varied between the initial and the final measurements. We concentrate on the pin subsystem. Table 1 shows the fitted values of the set of natural frequencies and Q-factors before (initial) and after (final) the noise tests. These tables show modest changes in frequencies except for the first pin mode, which altered significantly. By contrast the shifts in Q-factors are quite large. The exact physical origin of these changes is not clear, but it is possible that the various bolted connections in the pin system have 'shaken down' during the week of noise testing. Also, over the week of experimental testing, the pin assembly had to be unclamped (but not taken apart) and moved on the bench to allow re-calibration of the strain gauges.

The modal parameters for the disc are not shown here because there are many more modes and their variation between the two sets of measurements is smaller. The greatest difference in frequency and Q-factors are 6% and 26%, respectively. As will be seen, the net effect of these changes to the two subsystems is large enough to be significant for the squeal predictions.

There is an important point to note in this connection. Although the measured transfer functions and deduced modal properties varied somewhat over the week of testing, any variation during the short time taken by an individual squeal test (a matter of seconds) would be negligible. There is thus no reason to doubt the approximate validity of the theory based on linear, time-invariant systems.

3.3. The two sets of predicted zeros

Squeal predictions are obtained by computing the complex zeros of D and identifying which are unstable. Checking stability can be achieved graphically by plotting these zeros in the complex plane as root locus plots. With the conventions used in Ref. [2], unstable zeros are located in the bottom half-plane, i.e. those with negative imaginary parts.

Fig. 6 shows four of these root locus plots. These plots contain a lot of information, and require careful study to interpret. The top two (a,b) are the initial predictions whereas (c,d) shows the predicted zeros using the final transfer function measurements. Fig. 6(a) and (c) correspond to anticlockwise rotation of the disc as viewed from the pin, while Fig. 6(b) and (d) show the zeros when the disc rotates clockwise.

3.3.1. The structure of the plots

Each of these plots contain three types of symbols. The *uncoupled* pin modes are shown as crosses ($\times$), while those of the disc are shown as plus signs ($+$). Their imaginary parts are calculated from their natural frequencies multiplied by their damping factors. Naturally, these are all in the stable domain.

The black dots represent the zeros of D for a given value of the coefficient of friction. Although $\mu_\circ$ could be inferred from the contact forces measurement during noise tests, it was thought instructive to vary it 'artificially' over a somewhat wider (but plausible) range to study the sensitivity of the zeros to variations in friction. At the stage when D is computed within the program, a constant value of $\mu_\circ$ is specified. The calculation is repeated for a range of values of $\mu_\circ$ from zero to 0.7 in steps of 0.02. All these results are

Table 1
Table showing difference in natural frequencies (in Hz) and Q-factors between the initial and the final measurements for the pin subsystem

Frequency (Hz)				
Initial	22.2	952	2940	12706
Final	18.7	962	2930	12466
% difference	18	1	0.3	2
Q-factors				
Initial	390	400	440	340
Final	320	160	200	340
% difference	22	150	120	0

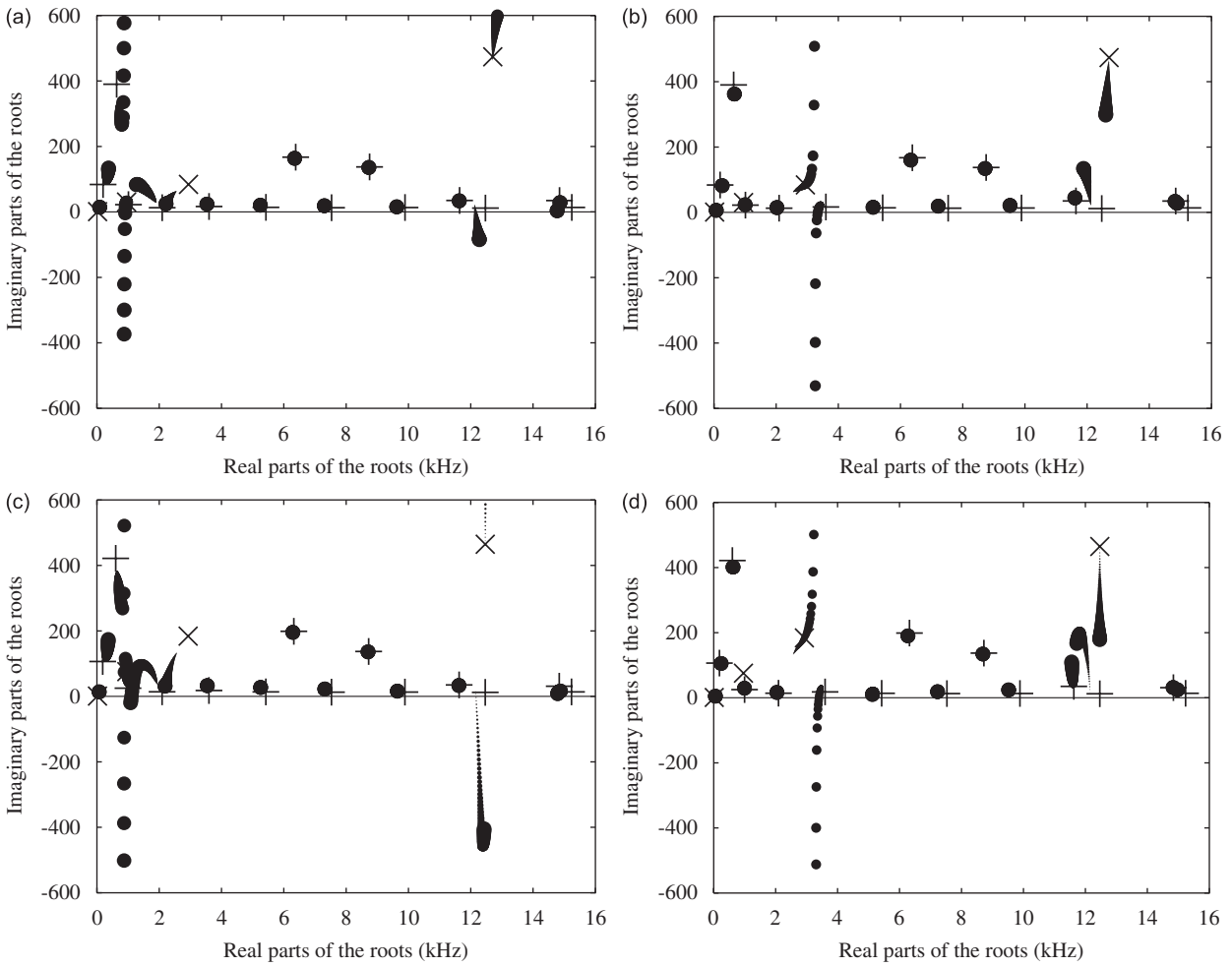

Fig. 6. Plots showing the predicted zeros of the coupled system in the complex plane for varying coefficient of friction values. For (a) and (b) the initial set of transfer functions were used; for (c) and (d) the final set. For each set, one plot is shown for each direction of disc rotation. In (a,c) the rotation is anticlockwise as viewed from the pin; in (b,d) the disc rotates clockwise. In each direction, the coefficient of friction was varied from 0 to 0.7. Increasing dot sizes correspond to increasing values of $\mu_\circ$. The plus and cross signs represent the uncoupled disc and pin modes respectively.

superimposed in the plot, with a symbol size which varied in proportion to $\mu_\circ$ so that the direction of variation can be seen. Thus, the gradient of symbol size gives a graphical illustration of how the zeros change when $\mu_\circ$ increases.

The vertical scale of the plot has been limited to allow a clearer display of the important features. Some extra zeros with large positive imaginary parts are thus not shown (this is why some of the larger dots appear to be missing in some strongly divergent branches).

3.3.2. Comments on the plots

One of the first noticeable features in these plots is that most of the zeros remain clustered together, showing as little blobs close to a disc mode (plus signs) or a pin mode (crosses). Examples of these appear in all four plots between say 4 and 12 kHz. However, other zeros move considerably as $\mu_\circ$ is varied. In some cases the change is slow enough that the plotted symbols overlap and produce thick lines, such as in (c) around 1 kHz. In some extreme circumstances, the sensitivity to $\mu_\circ$ is so great that the plotted points become widely spaced: for example the ones in the lower half-place of (b) around 3.5 kHz, or less dramatically the line of points around 12 kHz in (c). These widely spaced points indicate an effect of physical importance for this study.

They are often seen in regions where instability is predicted, and they indicate that the growth rate (and perhaps the stability threshold) is extremely sensitive to the value of the coefficient of friction. They are thus pointing to one possible source of the "twitchiness" of squeal.

Note that the smallest dots are always close to a disc or pin mode. This is to be expected because when friction is small, there is little coupling between the two substructures so that the coupled modes are close to the uncoupled ones.

It is important to bear in mind in looking at these plots that the main piece of information we are interested in are those zeros that cross the real axis downwards. For clarity, this information has been drawn out from the root locus plots and is presented in Table 2 which shows the frequencies of the unstable zeros together with the value of $\mu_\circ$ at which the zero crosses the real axis (thus becoming unstable). The layout of the table is the same as that of Fig. 6 so that a left–right comparison shows the effect on stability of changing the direction of the disc rotation whereas an up–down comparison shows by how much the predictions have changed between the initial and final measurements. The frequencies given in the table are those occurring at the crossing. As most unstable zero branches are close to vertical, the frequency range spanned as $\mu_\circ$ increases further is always fairly small.

From Fig. 6(a,c) and the corresponding cells in Table 2 (anticlockwise rotation), it appears that the two zeros initially predicted unstable have become three after the week of measurement. The initial 920 Hz unstable frequency has split into a pair at 825 and 1110 Hz. However, this 1110 Hz zeros only becomes unstable at the highest value of $\mu_\circ$ investigated here so that it is extremely difficult to see clearly this zero branch crossing the real axis on Fig. 6(c). The initial 12 150 Hz zero becomes unstable for even smaller values of the coefficient of friction.

When the disc rotates in the clockwise direction (Fig. 6(b,d)), the unstable zeros look very similar whichever of the two sets of measurements is used. Both show a single but strongly unstable zero around 3200 Hz, crossing the stability threshold for similar values of $\mu_\circ$. If $\mu_\circ$ is increased as high as 0.91 (not shown in Fig. 6), an extra unstable zero appears at 5085 Hz in the final set. By contrast, increasing the value of $\mu_\circ$ does not result in the creation of any extra unstable zero with the initial set.

Qualitatively, these predictions support well the theory presented in Ref. [2]. First, as a general rule, the larger the value of the coefficient of friction, the more unstable zeros are expected. Second, the modal density of the disc is much higher than that of the pin; therefore, wherever there is a pin mode, it is likely to be surrounded by two disc modes. If the residue of the corresponding pole in D for this pin mode is positive then a cluster of three modes with residues of alternating signs is formed, which was shown in Ref. [2] to be a condition for instability for well isolated three-mode clusters. The form of these residues is such that it is inevitable that a positive value can be achieved for one rotation direction or the other (but not both), provided the coefficient of friction is sufficiently big. The choice depends on the sign of the corresponding residue in H_{12}. The result is that the unstable zeros are more likely to appear near the pin modes. This is what is observed here: the predicted unstable zeros at 920/850, 3325/3385 and 12 150/12 150 Hz are all close to the pin subsystem natural frequencies: 960, 2930 and 12 460 Hz.

The sensitivity of squeal prediction to the modal parameters revealed in Table 2 may be related to the sensitivity of friction-induced vibration in general. The squeal frequencies predicted by the theory [2] only depend on the dynamical properties of the subsystems and the coefficient of friction. The "capriciousness" of friction-induced noise is almost always attributed to the inconsistency of the frictional element (i.e. the

Table 2
The frequencies of the unstable zeros and the corresponding threshold values of $\mu_\circ$ for the two sets of measurements and disc rotations

	Anticlockwise	Clockwise
Initial	920 Hz ($\mu_\circ \geqslant 0.66$) 12 150 Hz ($\mu_\circ \geqslant 0.1$)	3325 Hz ($\mu_\circ \geqslant 0.48$)
Final	825 Hz ($\mu_\circ \geqslant 0.64$) 1110 Hz ($\mu_\circ \geqslant 0.7$) 12 150 ($\mu_\circ \geqslant 0.01$)	3385 Hz ($\mu_\circ \geqslant 0.4$) 5085 Hz ($\mu_\circ \geqslant 0.91$)

tribology). Variation in the coefficient of friction can undoubtedly be a source of capriciousness. However, the variations in dynamic properties are seldom mentioned in this respect. Repeated measurements on the experimental rig over the duration of this work showed that the mechanical properties of the subsystems can vary significantly too.

Another issue relating to "capriciousness" concerns what constitutes a "good" measurement from a theory-testing point of view. An example will illustrate this: from the symmetry of the rig, the torsional modes of the steel strip of the pin assembly should not be excited so that the pin transfer functions should not have any peak at those torsional mode frequencies. With great care, it is possible to control the alignment so that hardly any sign of these modes appears in the transfer function measurements. However, during a squeal test, such precise positioning is almost impossible to achieve: the position of the pin subsystem relative to the disc is only approximately controlled and virtually impossible to repeat to the accuracy necessary to obtain repeatable measurements for the transfer functions. The problem of deciding which modes to include in the function D is critical—should those one would expect from a perfect measurement be chosen or those obtained from an approximate positioning more representative of a practical situation? In this paper, the former choice has been made. However, this issue of sensitivity to such things as alignment is an important one, and is the subject of continuing research.

4. Squeal tests

This section shows some results from the set of squeal tests carried out during the week of measurement. The objective is to illustrate how the experimental data was exploited for the purpose of testing the theory presented in Ref. [2] and also to present some of the difficulties encountered in doing so.

Each test consisted of running the disc with a given speed and direction and applying the pin with a given normal preload. If any squeal event occurred, the normal and friction forces together with a microphone signal of the radiated sound were recorded by digital data-logger. For each test, the signals were recorded for 5 s. The tip of the pin always made contact with the disc at the exact radius where the transfer functions for the disc were measured. A full set of squeal tests, carried out on each day of the week of testing, consisted of six cases: disc speeds of approximately 3, 7 and 15 rev/min were used, in both clockwise and anticlockwise directions.

If the pin was first preloaded on the disc at rest, then the disc set into motion, the pin usually went through a stick–slip regime at very low speeds. Since the theory to be tested here relates only to the prediction of linearised stability thresholds, it was undesirable to start each test with complex nonlinear vibration. To avoid this problem, the disc was first set to the required rotation speed, then the pin was pushed against the disc using the preloading spring. This eliminated the initial occurrence of stick–slip. Even with such careful procedures, it was not always easy to decide what constituted a 'typical' squeal event, one worth recording. However, after a few preliminary runs the rig would behave in a fairly consistent manner within a time interval of two hours or so, provided the settings were all unchanged.

One illustrative case has been chosen for detailed discussion. This squeal test was carried out on the *Day 1* of the week of tests, with anticlockwise rotation at 7 rev/min. Fig. 7 shows the data obtained in four plots.

The two plots at the top are raw time series: the very top one shows the microphone signal while the second plot from the top shows time histories of the calibrated normal (grey, bottom curve) and tangential (black curve) forces. The next plot down (i.e. in third position from the top) shows the time history of the coefficient of friction deduced from the data of the middle plot. The plot at the very bottom of the figure is a time–frequency graph (sonogram) obtained by processing the microphone signal using a short time Fourier transform and Hanning window. The result from this processing is an array of amplitudes indexed by time and frequency indicating the timing and approximate frequency of "noise events" captured in the recording. The size of each FFT was 4096 sampled points, 1.67% of the total record length. The sampling frequency was 50 kHz per channel. The plot is a pixel image of the amplitude matrix such that the darker the image cell, the higher the amplitude. Therefore noise events appears as darker regions. A single-frequency squeal event would show up as a horizontal dark line: the best example in this plot is indicated by an arrow as discussed below. All four plots are aligned vertically so that the time axis is the same.

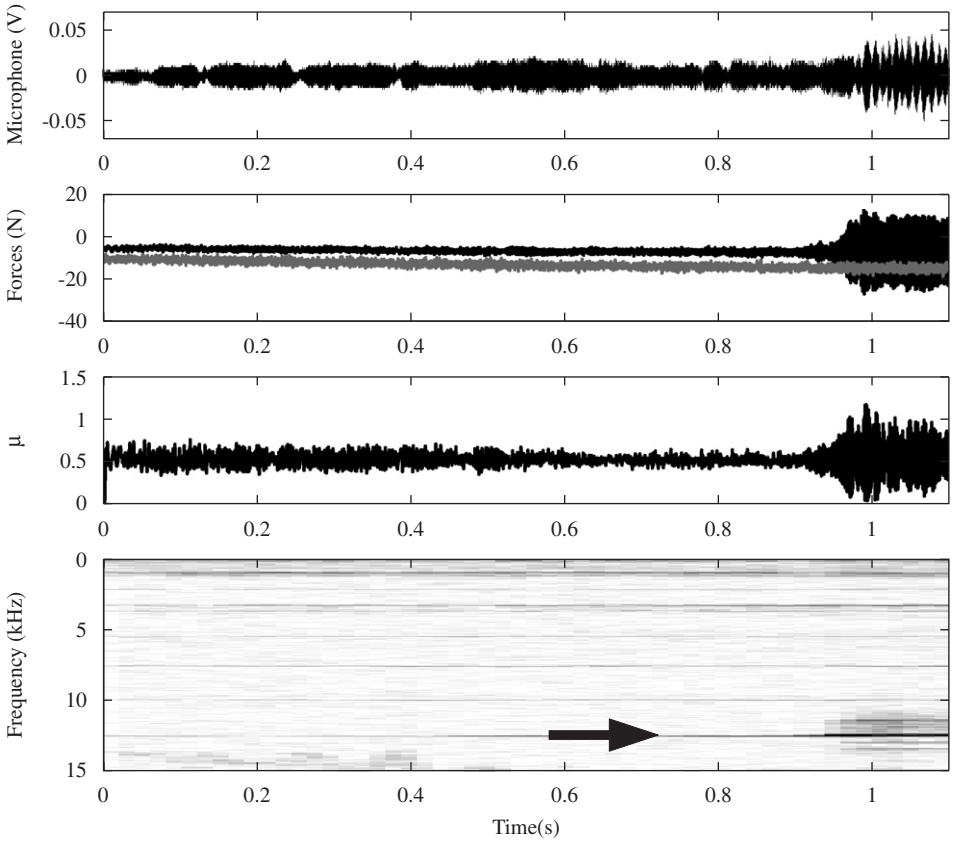

Fig. 7. Set of four plots showing (top) the time history of the microphone signal during the noise initiation phase, the time histories of the calibrated normal force (grey, bottom curve in the second plot from the top) and friction force (top black curve in the same plot), the time history of the coefficient of friction deduced from the forces (in the third graph from the top) and a sonogram of the microphone signal (bottom graph). The disc was rotating anticlockwise at 7 rev/min.

The sign of the forces as measured are arbitrary as they result from the way the gauges were wired. The slow variation in the normal force is due to slight misalignment of the disc with the main axis of the motor, causing an out-of-plane displacement of the disc of a few tenths of a millimeter so that the normal load varies somewhat as the disc rotates. The frequency concerned is less than 1 Hz, so the variation is slower by several orders of magnitude than the typical squeal oscillations, and it seems in order to treat it as quasi-steady and continue to use the constant-force theory for interpretation. It can be observed that the friction force varied more or less in proportion, so that the coefficient of friction remains remarkably constant at an average of 0.60 throughout the noise initiation. Over the week, the (average) values of $\mu_\circ$ were found in the range 0.4–0.7 for perspex on aluminium, so that the value seen here lies towards the upper end of the range.

Fig. 7 only shows the data up to 1.1 s because after that time the squeal evolved into a very loud noise, and loss of contact between pin and disc occurred. The system then settles in a highly nonlinear regime which the theory presented earlier [2,3] is not expected to model. Even for the moderate amplitudes seen in the time range plotted here, it is not obvious how accurate linearised theory will be. This is an important subject for further research. However it should be noted that within the time shown, the amplitude of the microphone signal is very small.

The top plots shown in Fig. 7 suggest that nothing noteworthy occurs before $t = 0.9$ s. Around that time, oscillations start to grow, most obvious in the friction force trace. This initial growth is the most important part for testing a linear theory, therefore this is the region of the data that will be compared with the prediction in the next section. The sonogram is difficult to interpret in these small black and white plots, and a little effort is needed from the reader. There are several faint frequency lines running intermittently in the background but

the dominant event is a ridge at 12 450 Hz starting from 0.9 s onward and indicated on the plot by a thick black arrow. Therefore, this frequency was selected as the main initial squeal frequency component for this test.

5. Comparison with prediction and discussion

The results obtained during the week of testing are summarised in Table 3. This table shows the incipient squeal frequency(ies) in Hertz for a given day at a given speed (in rev/min). Frequencies up to 15 kHz are reported except for Clockwise 3 rev/min on *Day 1* where the first frequency to appear was at 15 250 Hz. The frequencies printed in bold are the experimental squeal frequencies for which there is a fairly close theoretically predicted unstable zero (within 10–15%). Within this uncertainty range, 73% of squeal frequencies recorded were predicted (i.e. the squeal frequencies in bold represent 73% of the noise frequencies observed and reported in the table).

In order to investigate the influence on the squeals generated of the exact position of the pin subsystem with respect to the disc (alignment, etc), the tests carried out on Days 2, 3 and 4 were conducted without dismantling the pin (these three days are written in italic in the table to distinguish them from the other days). Comparing tests on Days 2, 3 and 4 together, it appears that for a given disc speed, their squeal frequencies are very similar. In the anticlockwise direction, they are identical. For clockwise rotation, there are more discrepancies but the results are nevertheless fairly similar. Comparing this subset of results with those of the initial and the final days, more discrepancies arise. Taking the pin apart from the disc and mounting it again could influence the system via different routes: (1) the location of the contact point is not exactly the same, thus changing the friction characteristics and/or slightly shifting the natural frequencies; (2) some differences in the tightening of the bolts could induce some variation in the associated interfacial damping. However, the appearance of the new 5500 Hz squeal at 15 rev/min clockwise in the test from Days 3, 4 and 5 suggests that the system properties evolve even if no apparent changes are made to it.

The different set of squeal frequencies when the disc rotates clockwise and anticlockwise confirms that the asymmetry introduced in the pin assembly had the expected effect. As pointed out in Ref. [1], changing the disc rotation amounts to mathematically change the sign of $\mu_\circ$ in Eq. (1). Physically, it illustrates the fact that if the pin does not push on the disc symmetrically, then it will be 'trailing' in one disc direction and 'digging-in' in the opposite direction.

The velocity appears to have a significant effect. First, different frequencies can appear for different speeds on a given day. Most are approximately as predicted, but some may not be. Qualitatively, it appears that the velocity has an influence on which frequency is being "picked" to be unstable. For instance, at 3 rev/min anticlockwise, the 940 Hz squeal is predominant on most days, whereas at 7 or 15 rev/min, 12 500 Hz is. The theory presented [2] cannot account for any velocity effect. However, using the theory presented in Ref. [3] with a coefficient of friction linearly varying with sliding speed, it might be possible to predict these changes. The role of the normal load previously described supports this suggestion. This is the subject of continuing research.

Table 3
Table showing the squeal frequencies (in Hz), measured from noise tests on different days for different disc speeds

	Disc speed (rev/min)	Prediction 1	Day 1	*Day 2*	*Day 3*	*Day 4*	Day 5	Prediction 2
Anticlockwise	3	850 12 700	**940**	**940**	**940**	**940**	**940 + 12 500**	850 11 500/12 500
	7	850 12 700	**12 500**	**12 500**	**12 500**	**12 500**	**12 500**	850 11 500/12 500
	15	850 12 700	**12 500**	**12 500**	**12 500**	**12 500**	**10 000**	850 11 500/12 500
Clockwise	3	3200	15 250	12 500	**2750** + 12 500	**2600** + 12 500	**2800** + 10 000	3300 4900/5500
	7	3200	**2700** + 12 500	**2700**	12 500	**2700** + 12 500	**2800 + 5500**	3300 4900/5500
	15	3200	**2800** + 12 500	**2700**	**2700 + 5500**	**2700 + 5500**	**2750 + 5500**	3300 4900/5500

The test numbers, in the first row, are in chronological order. The predicted unstable frequencies have been added in an initial and final column. The experimental frequencies printed with a bold font are the observed noise frequencies close to a predicted ones.

6. Conclusion

This paper describes an experimental investigation aimed at testing the validity of a theory presented in two earlier papers [2,3], concerned with the prediction of instability arising when two systems slide against each other at a single contact point. The aim of the present experimental study is limited to the testing of the simplest theory presented in Ref. [2], where the coefficient of friction characterising the interface is assumed to be constant. The predictive scope of this theory is restricted to linear behaviour, so that only squeal initiations are expected to be predicted accurately.

For the purpose of validation, a pin-on-disc rig was used. Friction-induced vibration experiments offer notoriously bad repeatability and this rig was no exception. In order to present a systematic investigation, the squeal results presented here were obtained over a week of measurement. This was to ensure that the natural evolution of the rig dynamics with time was kept to a minimum. Transfer function calibration measurements were carried out once before the 5 days of squeal runs and once after. This showed that small variations in the dynamics of the system could cause different squeal frequencies to be predicted unstable. The 'capriciousness' of friction-induced vibration phenomena is often attributed to the transient properties of the frictional interface (such as wear of the oxide layers, temperature rises...). While this study has shown that the threshold of instability can indeed be sensitive to the value of the coefficient of friction, it also shows that some of the variation in the instability can be attributed to slight changes in the dynamic properties of the systems in contact. It is also important to realise that the capriciousness is also encountered numerically, without the introduction of any nonlinear feature in the model so that it cannot be attributed to any "butterfly effect".

Comparison between predicted unstable frequencies and experimentally observed squeal frequencies revealed that more than 70% of the noise occurrences could be approximately predicted with the theory using a constant coefficient of friction. One prediction is quite well supported by the test: on the whole, the squeal frequencies are different when the disc rotation is reversed. Results from the squeal tests however suggest the squeal frequencies are influenced by the magnitude of the sliding velocity as well. Such an effect cannot be accounted for by the theory tested here but it points to the extension of the model made in Ref. [3], where it was shown that the stability criterion becomes dependent on the sliding speed when the coefficient of friction is no longer assumed to be constant. Continuation of this experimental study is under way to allow this extended theory to be tested.

Acknowledgements

The authors thank Bosch Braking Systems for financial support, Professor K. L. Johnson and Dr. Derek Smith for valuable discussions and the team of technicians from Mechanics Laboratory of the Cambridge University Engineering Department for their skilful work.

Appendix A. Overall diagram of the set-up

A diagram showing the disc sybsystem (left) in contact with the pin subsystem (right) is given in Fig. 8.

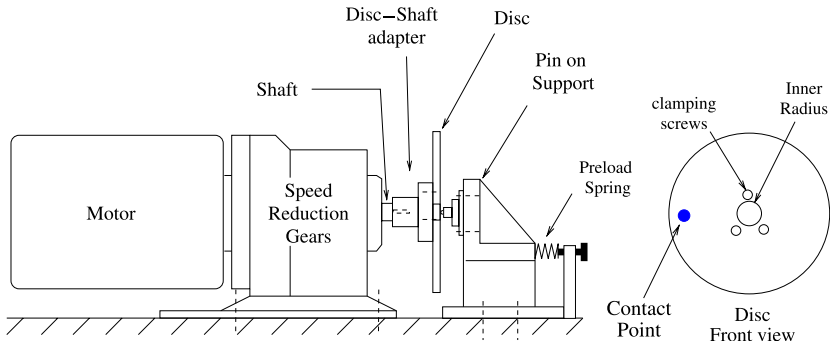

Fig. 8. Diagram showing the disc subsystem (left) in contact with the pin subsystem (right).

References

[1] K.L. Johnson, Tribology research: from model experiment to industrial problem, in: G. Damaz, A.A. Lubrecht, D. Dowson, M. Priest (Eds.), *Tribology Series Proceedings of the 27th Leeds-Lyon Symposium on Tribology INSA*, vol. 39, Elsevier Science Dynamic friction, Lyon, 2001.
[2] P. Duffour, J. Woodhouse, Instability of systems with a sliding point contact. Part 1: basic modelling, *Journal of Sound and Vibration* 271 (2004) 365–390.
[3] P. Duffour, J. Woodhouse, Instability of systems with a sliding point contact. Part 2: model extensions, *Journal of Sound and Vibration* 271 (2004) 391–410.
[4] J.D. Smith, *Vibration Measurement and Analysis*, Butterworths, London, 1989.
[5] J.W.S. Rayleigh, *The Theory of Sound*, vol. 1, Dover, New York, 1945.
[6] M.R. North, Disc brake squeal—a theoretical model, M.I.R.A. Research Report 1972/5, 1972.
[7] J.E. Mottershead, S.N. Chan, Flutter instability of circular discs with frictional follower loads, *Transactions American Society of Mechanical Engineers, Journal of Vibration and Acoustic* 117 (1995) 161–163.
[8] E. Skudrzyk, *Simple and Complex Vibratory Systems*, Pennsylvania State University Press, 1968.
[9] P. Duffour, Modal testing on violin bodies, Cambridge University Engineering Department, Technical Report, 1998.
[10] S. Adhikari, Damping Models for Structural Vibration, PhD Thesis, Cambridge University Engineering Department, 2000.
[11] D.J. Ewins, *Modal Testing*, second ed., Research Studies Press Ltd., 2000.